Journal of Natural Resources and Environmental Management
http://dx.doi.org/10.29244/jpsl.14.4.684

RESEARCH ARTICLE

OPEN ACCESS

Check for updates

Evaluation of Floods Susceptibility Models Based on Different Pairwise Parameters in the Analytical Hierarchy Process: Case Study Cilemer and Ciliman Watersheds

Dian Noor Handiani, Ditto Purnomo

Program Study of Geodetic Engineering, Faculty of Civil and Planning Engineering, National Institute of Technology, Bandung, 40124, Indonesia

Article History
Received
30 November 2023
Revised 20 March 2024
Accepted 05 June 2024

Keywords
AHP, floods, pairwise parameters, watershed

ABSTRACT

This study investigated flood vulnerability in the Ciliman and Cilemer Watersheds, situated in Banten Province, and employs a spatial multi-criteria-integrated approach, with a specific focus on the Analytical Hierarchy Process (AHP). Two distinct scenarios, which have different parameter priority, were compared: one based on expert judgment for pairwise parameter comparisons (scenario-1) and the other derived from historical flood occurrences in high and very high vulnerability areas (scenario-2). Seven parameters, including elevation, slope, precipitation, geologic, soil type, land use, and distance to streams were weighted substantially different between the two scenarios. The study validated the flood vulnerability scenarios by contrasting them with historical flood data. Scenario-2 exhibited a closer agreement with the historical flood points during validation, particularly in very high vulnerability areas. Elevation and slope are identified as pivotal factors influencing flood vulnerability: low elevations and gentle slopes increased vulnerability, while higher slopes decreased flood susceptibility.

Introduction

The ignoring principle of land conservation on land use change and agricultural land processes is one of the drivers of decreasing watershed hydrology function. The reduction is shown by the inability of the watershed to control water fluctuations due to large surface runoff during high precipitation or water supply during the dry season [1]. This means that land-use change and its transformation over time are the most influential factors in the hydrological budget, such as evaporation, surface runoff, infiltration, and groundwater recharge [2]. This condition can worsen when climate extremes (e.g., high precipitation) occur.

Extreme climates lead to heavy rainfall, which, along with land use change, is one of the factors that influence flood occurrence in a watershed region. Although floods are natural phenomena caused by natural events and human activities [3], their occurrence could potentially cause injury to humans and environmental damage. Hence, mapping and assessing flood potential areas is crucial, as they provide essential information for setting up priority actions to control flood occurrence in watershed areas [4]. Furthermore, the map and assessment can contribute to mitigating the impacts of floods on people, property, and the environment. The maps produced can also be used by policymakers for effective management plans targeting prevention and reduction measures [5].

Flood occurrences in the Ciliman and Cilemer Watersheds, as part of the Pandeglang and Lebak Regencies of Banten Province, are becoming more frequent. Data from the National Agency for Disaster Management/ *Badan Nasional Penanggulangan Bencana* (BNPB) showed that there were thirty-one locations of flood occurrences between 2010 and 2020 [6] in the Ciliman and Cilemer Watersheds, with a frequency of occurrence of at least once a year. The Regional Agency for Disaster Management/*Badan Penanggulangan Bencana Daerah* (BPBD) of Serang City stated that flooding in the Ciliman Watershed was caused by the

Corresponding Author: Dian Noor Handiani ddhandiani@itenas.ac.id Study Program of Geodetic Engineering, Faculty of Civil and Planning Engineering, National Institute of Technology, Bandung, Indonesia.

© 2024 Handiani and Purnomo. This is an open-access article distributed under the terms of the Creative Commons Attribution (CC BY) license, allowing unrestricted use, distribution, and reproduction in any medium, provided proper credit is given to the original authors.
Think twice before printing this journal paper. Save paper, trees, and Earth!

overflow of the Ciliman tributaries. The overflow was caused by high precipitation and the inability of the ground to absorb rainwater properly, which caused the overflow to go directly into runoff [7]. Therefore, a map of the potential spatial flooding areas is necessary.

Many studies have developed a spatial multi-criteria-integrated approach of potential flood area mapping using geospatial techniques at the local scale [5,8,9], and they used the Analytical Hierarchy Process (AHP) calculation as one of the Multi-criteria decision-making (MCDM) Methods. In the AHP calculation, the weight priority parameters are estimated from a pairwise comparison according to nine level scales [10]. The comparison requires expert judgment, and in practical cases, experts might not be able to determine numerical values because of their limited understanding or capability [11].

This study was undertaken to compare two potential flood-vulnerable areas of the Ciliman and Cilemer Watersheds in the Pandeglang and Lebak Regencies of Banten Province. In comparing the two scenarios of potential flood-vulnerable areas within the Ciliman and Cilemer Watersheds of Pandeglang and Lebak Regencies in Banten Province, several aspects were examined. First, the methodology employed in each scenario, particularly the differences between using pair-wise comparison based on expert judgment found in earlier studies by BNPB [12] and Ramadhani et al. [13] versus data-driven comparison based on historical flood points during validation, particularly in highly vulnerable areas of the flood vulnerability parameter, will be assessed. This includes the evaluation of the reliability, accuracy, and robustness of the AHP method in both scenarios. Second, the resulting flood vulnerability maps generated from each scenario were compared in terms of spatial extent, severity of vulnerability, and identification of high-risk areas. Additionally, the factors considered in the pair-wise comparison, such as elevation, slope, precipitation, geologic, soil type, land use, and distance to stream variables, were analyzed to understand their influence on the differences observed between the two scenarios.

Materials and Methods

Study Area

The study areas, the Ciliman and Cilemer Watersheds, are located in Banten Province, Java Island. The Ciliman Watershed has an area of 527 km^2 and a length of 55 km [7], while the Cilemer Watershed has an area of 577.2 km^2 and a length of 22.8 km [14]. These two watersheds are in Pandeglang and Lebak Regencies in the western part of Banten Province, as illustrated in Figure 1.

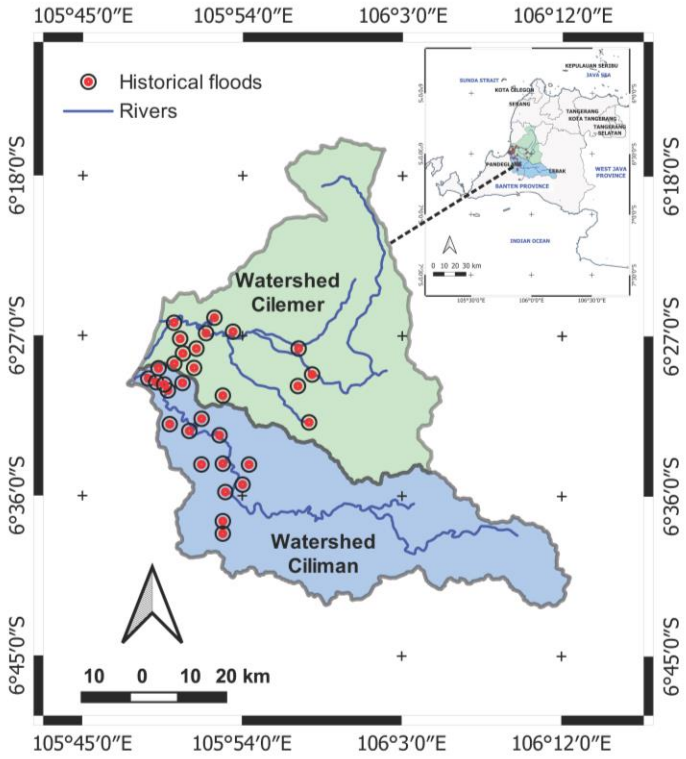

Figure 1. Study area with spatial distribution of historical floods (red dots on the map).

Most of the Cilemer Watershed is lowland (0–25 m) (77.38% of the total area) [15]. This factor and the different capacity between upstream and downstream watersheds, as well as increased water discharge of the river tributaries area, are some of the reasons why flooding occurs in the area [16]. Meanwhile, in the Ciliman Watershed, overflow of the Ciliman tributaries is caused by land use conversion upstream of Ciliman [7]. In our research, 30 flood occurrences were identified in these watersheds (red dots in Figure 1), based on historical data from Indonesia's disaster data information (https://gis.bnpb.go.id accessed on 26 August 2024) and the BNPB. The flood occurrence data were collected between 2010 and 2020.

Dataset and Sources

This study used seven parameters related to flooding for the calculation and analysis process: elevation, slope, precipitation, geologic and soil type, land use, and distance to streams. These parameters were suggested by Ramadhani et al. [13] and were selected by considering the natural characteristics of the regions [15]. Cagla and Leyla [17] indicated variability in the number of parameters used in mapping potential floods, ranging from a maximum of 21 to a minimum of five preferred parameters. Despite this variability, certain parameters were found to be predominant across studies. The parameters used in this study were among the dominant parameters used in many studies. The data were collected from several sources, and are presented in Table 1. Thematic and geometric editing, spatial manipulations, and simple basic calculations (e.g., buffer zones around streams and interpolation of precipitation data) were applied to the selected parameters when preparing them for integration in the spatial dataset. All parameters were processed in the Geographic Information System (GIS) environment as vector layers with the lowest scale map of 1: 250,000.

Table 1. Data used and source.

Parameter	Scale/resolution	Data format	Data source
Elevation (%)	0.27-arcsecond	Raster	Digital Elevation Model National (DEMNAS) and Geospatial Information Agency/*Badan Informasi Geospasial* (BIG)
Precipitation (mm)	0.05°	Vector (points)	The Climate Hazards Group Infrared Precipitation with Stations (CHIRPS)
Geologic map	1: 100,000	Vector (polygon)	Geological Research and Development Centre
Soil type	1: 250,000	Vector (polygon)	Digital Soil Map of the World-ESRI
Land use	10 m	Raster	Sentinel-2 10 m Land Use/Land Cover Time Series
Distance to stream (m)	1: 25,000	Vector (lines)	BIG
Flooding occurrences		Vector (points)	BNPB

Method Data Processing and Analysis

The workflow illustrated in our study (Figure 2) consists of the following major steps: 1) data collection and storage, 2) data processing, 3) assessment of vulnerability parameters according to the vulnerability rank (Table 2), 4) applying the AHP framework, and 5) calculation and mapping of flooding vulnerability. In step 4, the AHP framework calculation process revealed three important parts: hierarchy development, pairwise components, and synthesis of priority [18,19]. There are two scenarios in the calculation and mapping of Steps 4 and 5 (black dashed lines in Figure 1). The scenario differs within step 4 (blue dashed lines in Figure 2), with the hierarchy development in scenario 1 being based on earlier study/expert judgment, while scenario 2 was based on a comparison between each parameter's vulnerability and flooding occurrences. The parameter with the highest number of flooding occurrences has the highest priority compared to the other parameters. Each scenario generated its own priority list of flooding parameters; hence, each parameter weight had a different value in each scenario.

First, we collected and stored data (Table 1). Second, the parameters were preprocessed. Third, each parameter was ranked into five categories on a scale of 1 to 5 (low risk to high risk) (see Table 2). The process is then divided into two scenarios. This scenario differs from the AHP framework assessment. Each scenario has a different process for developing the parameter hierarchy. Then, pair-wise comparisons were performed, with each scenario producing different results. Although the matrix process (pairwise) was the same, the scores were based on their relative importance for each scenario. In the construction of the matrix, each parameter was rated against every other factor by assigning a relative dominant value between one and nine (Table 3).

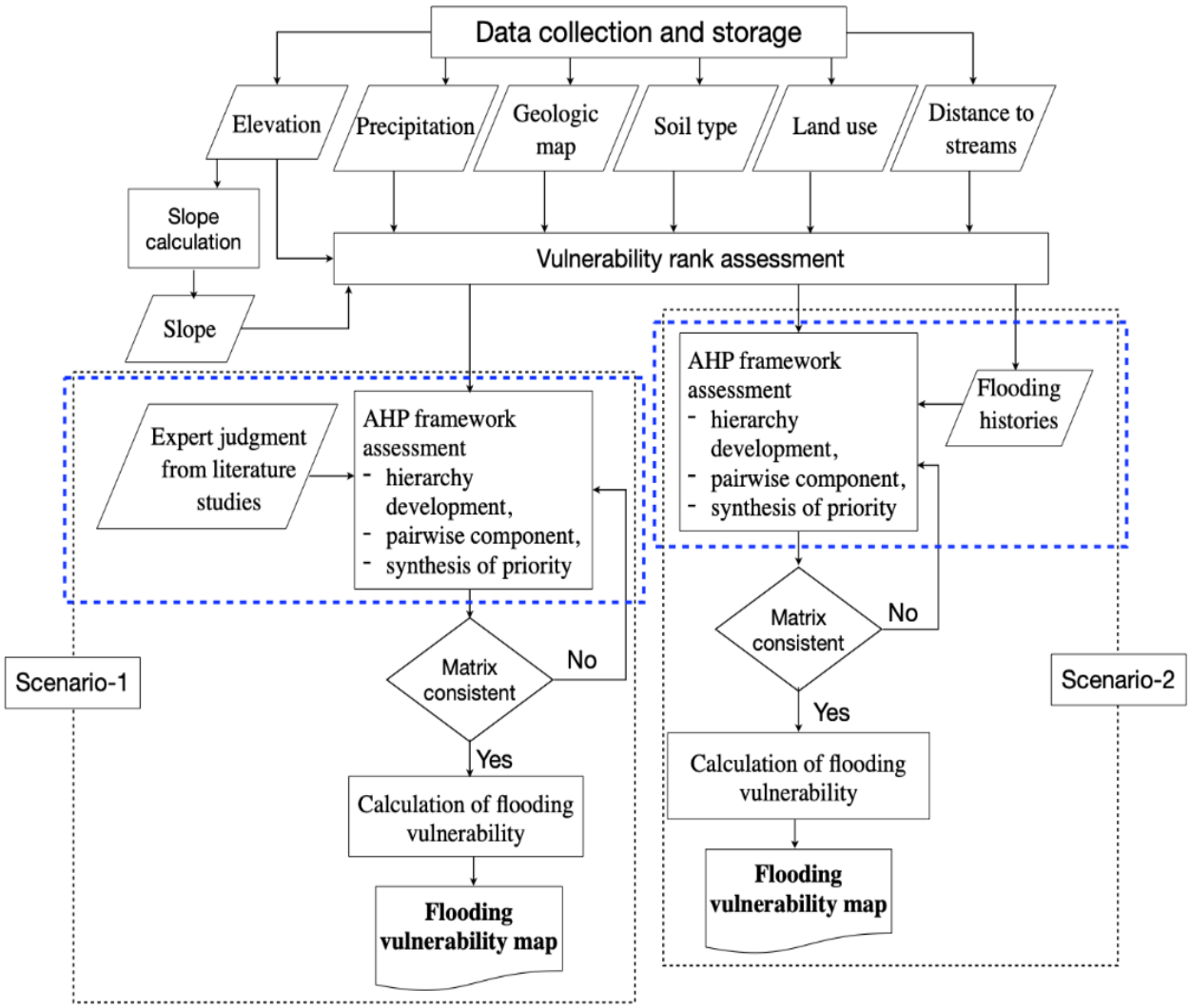

Figure 2. Flowchart methodology.

Table 2. Vulnerability scoring of parameters.

Parameters	Vulnerability rank (score)				
	1 (Very low)	2 (Low)	3 (Moderate)	4 (High)	5 (Very high)
Elevation (m)	> 200	101–200	51–100	20–50	0–20
Slope (%)	> 45	25–45	15–25	8–15	0–8
Precipitation (mm year^{-1})	< 1,000	1,000–1,500	1,500–2,000	2,000–2,500	> 2,500
Geologic	Andesite, basalt, clay rock, Badui formation (Tmd), Cipacar formation (Tpc), Genteng formation (Tpg), lava volcano rock	Sandstone, quaternary volcanic rocks	Limestone, coral, Cihowe formation (Tmc)	Bojong formation (Qpb), Bojongmanik formation (Tmb)	Alluvium (Qa)
Soil type	Regosol, lithosol, organosol, rendzina	Podzolic, podzol, andosol, grumosol	Brunisolic, alfisol	Lathosol	Alluvial
Land use	Forest	Swamp, lake, fishpond	Open landscape	Agriculture land	Built-up area
Distance to streams (m)	> 600	600	450	300	150

Source: Adapted from Ramadhani et al. [13].

Table 3. Analytical Hierarchy Process (AHP) rating scale.

Scale importance	Definition	Explanation
1	Equal importance	Two parameters contribute equally to the object
3	Somewhat more important/moderate importance of one over another	Experience and judgement slightly favour one over the other
5	Much more/essential important	Experience and judgement strongly favour one over the other
7	Very much more important	Experience and judgement very strongly favour one over the other
9	Extreme importance	The evidence favouring one over the other is of the highest possible validity
2, 4, 6, 8 (reciprocals)	Intermediate values between the two	When compromise is needed

Source: Handiani et al. [18].

Each matrix in the scenario was examined for consistency by calculating a consistency index. This index is known as the consistency ratio (CR) and is used in the AHP synthesis process [18]. The CR was computed using Equation (1). When CR is > 0.10 (10%), the comparison matrix indicates inconsistency, and the matrix needs to be readjusted with different pairwise comparisons according to [18].

$$CR = \left(\frac{CI}{RI}\right) < 10\% \quad (1)$$

where CI is the consistency index, and RI is a random index for different values of n (see Equation 2). The random index (RI) depends on the number of components in the comparison matrix. When the number of parameters was seven, the RI value was 1.32.

$$CI = (\lambda_{max} - n)/(n - 1) \quad (2)$$

where λmax is the largest or principal eigenvalue of the matrix and n is the order of the matrix. In this study, if the CR value was < 0.10, the computation was accepted, indicating reasonable accuracy for the pairwise comparison matrix.

In the later phase, the flooding vulnerability map was visualized based on the calculation of flooding vulnerability. The calculation is the integration of all the parameter ranks and their weights, which was formulated as (Equation 3):

$$FVI = \sum_{i=0}^{n}(r_i * w_i) \quad (3)$$

where FVI is the flood vulnerability index, ri is the rank of the parameters, w_i is the weight value of each parameter, and n is the number of factors. All processes and calculations were performed using GIS. The calculated FVI was ranked into five categories: very low, low, moderate, high, and very high vulnerability. These categories were represented by equal count (quantile) FVI percentile ranges of 0–20%, 20–40%, 40–60%, 60–80%, and 80–100%. The two scenarios led to a vulnerability map as the final output of the flooding vulnerability assessment.

Results and Discussion

Flooding Parameters Vulnerabilities

In this study, multi-source geospatial parameters were used to prepare a flood vulnerability map: elevation, slope, precipitation (rainfall), geologic, soil type, land use, and distance to streams. The parameters were ranked from 1 to 5 according to the classifications in Table 2. The results of this classification showed how each parameter within the spatial area could potentially contribute to the flood. The higher the value (or rank), the higher is the contribution of the parameter to flood occurrence in the area. Finally, each parameter was classified into five ranks: very low, low, moderate, high, and very high. The overall visualization is shown in Figures 3.

Water flows from higher elevations to lower flat lowland areas. This means that flat lowlands may flood faster than areas with higher elevations [20–22]. The elevation map in Figure 3a shows that the highest potential flood area is in a flat area west of the study area (estuary), and the flood potential continues at a lower risk to the east side of the study area. The flooding history also showed that most flooding occurrences were related to the parameter with the highest rank (30 locations from a total of 31 locations). Furthermore, the

slope of an area plays a fundamental role in regulating surface discharge, and it becomes a very important topographic factor [23]. The stiff slope can be correlated to an area of high surface flow velocity [24]. In Figure 3b, the slope is dominant at very low values in almost all study areas, whereas the highest and highest values are in the western part of the study area. Hence, comparing the flooding history with this parameter showed that only three locations out of a total of 31 locations are in high and highest flooding potential areas.

Figure 3c shows the rainfall parameter classification for flood potential mapping. There are only two representations of the values: high and very high. This means that rainfall had a value of more than 2,000 mm yr^{-1} in the study area. This rainfall map was prepared based on point rainfall data for one year (Figure 3c). Numerous studies worldwide [13,25,26] have selected rainfall as one of the principles that influences the components of flood potential mapping. Our study showed that all flooding histories occurred in areas with high or very high rainfall (Figure 3c).

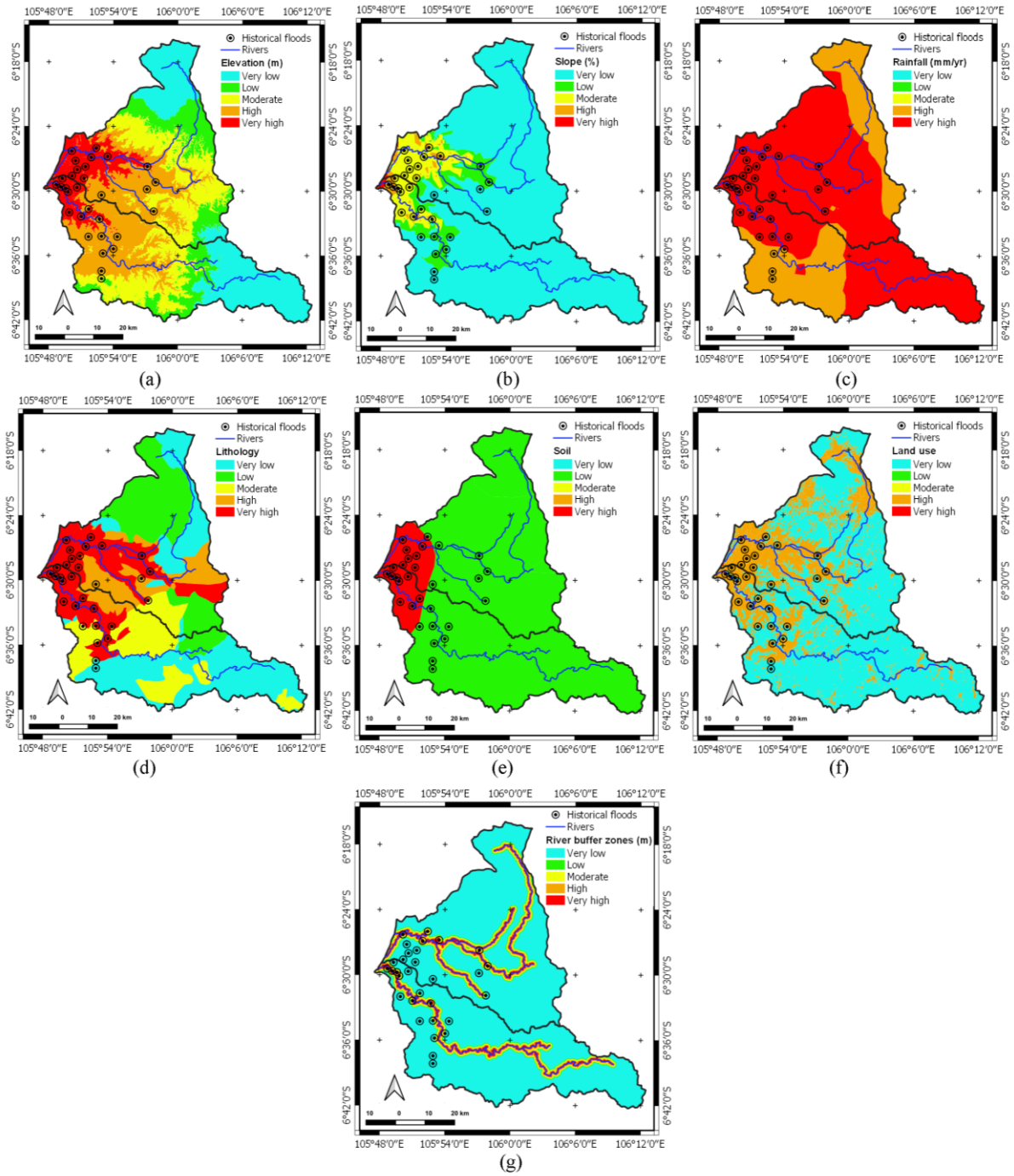

Figure 3. Maps representing flood control parameters; (a) elevation, (b) slope, (c) precipitation, (d) geologic, (e) soil type, (f) land use, and (g) distance to streams.

A geological (lithology) map of the Cilemer and Ciliman Watershed catchments was prepared based on the geological and rock types (Figure 3d). The geology of an area can provide substantial information on the occurrence of paleoflood events [27,28]. A geological formation with higher permeability will lead to a higher infiltration process, whereas an impermeable layer will increase surface runoff. In our study, high and very high are classified as alluvium (Qa), Bojong formation (Qpb), and Bojongmanik formation (Tmb), which are quaternary sedimentary rock types [29]. These areas are spread from the western to the eastern part of the study area (Figure 3d). Comparing the flooding history with this parameter showed that most occurrences were in high and highest flooding potential areas (29 of a total of 31 locations).

Soil type can determine the level of infiltration, which can influence flood vulnerability. The slower the land infiltration, the greater the surface flow, which results in flooding. In this study, soil-type maps were obtained from a digital soil map of the world from the FAO and UNESCO in 1961 at a 1: 250,000 scale. The classification of soil types as flood hazard parameters in our study is presented in Figure 3e, and is classified into two types: low and very high. This parameter was compared to the flooding history, and the results showed that 17 locations of flooding occurred in the very high soil type.

Figure 3f and 3g show the land-use pattern and distance from the stream network in the study area. According to García-Ruiz et al. [30], land use in an area is important for hydrological responses during different periods. Furthermore, Figure 3g shows the distance from the stream network, and it buffers the distance from the rivers between 150 and 600 m. Kourtis and Tsihrintzis [31] and Miranda et al. [32] found that the expansion of a flood event depends on the distance of a region from the drainage network. The closer the location of an area to the stream network, the more likely it is to suffer from flooding than in areas that are far away. A comparison of the flooding history with these parameters showed that 26 locations could be classified as having high and highest flooding occurrences, and only 12 locations with high and highest rank flooding occurrence classifications were at a distance from the stream network. Based on these contributor parameters of flood susceptibility, our study sorted these parameters from the highest to the lowest rank. Rainfall, elevation, lithology, land use, soil type, distance from the stream network, and slope were sorted for the pairwise comparison matrix.

The Pairwise Comparison Matrix and Weighted Parameters

AHP was developed by Handiani et al. [18] and is a practical multi-criteria decision-making technique. The multi-criteria decision is weighted based on their priority through pairwise comparison of alternatives. The pairwise comparison values of the decision elements are evaluated at each level of the hierarchy, and the values are then used to derive the priority weights of the parameters. Often, expert opinions are sought for pairwise comparisons. In our study, we compared two sets of pairwise values: one set was from an earlier study with expert opinion (scenario-1), and the second set was from the number of flooding occurrences in high and very high classifications of each parameter that supports flood susceptibility (scenario-2). Using these pairwise values, we can derive different weighted ranks of the parameters. Tables 4 and 5 are pairwise matrices for each scenario, whereas Tables 6 and 7 are normalized matrices for each scenario.

As described in Tables 4 to 7, we derived the weights of the parameters in scenario 1. The slope is 0.37, rainfall is 0.23, land use is 0.12, lithology is 0.11, soil type is 0.07, elevation is 0.05, and distance to streams is 0.04. The weighted parameters in scenario-2 were rainfall is 0.37, elevation is 0.21, lithology is 0.17, land use is 0.11, soil type is 0.07, distance to streams is 0.04, and elevation is 0.02. Both indices of CR were computed (using Equation 1), and both CR satisfied the condition (less than 10%), showing the consistency of the matrices. From these matrices, we obtained two sets of weighted parameters and sorted the list of flood-vulnerability parameters.

Table 4. Physical parameter for pairwise comparison matrix for scenario-1.

Parameter	Slope	Rainfalls	Land use	Lithology	Type of soils	Elevation	Distance to streams
Slope	1	3	3	4	5	7	7
Rainfalls	0.33	1	5	2	3	5	5
Land use	0.33	0.20	1	3	2	2	2
Lithology	0.25	0.50	0.33	1	3	3	3
Type of soils	0.20	0.33	0.50	0.33	1	2	2
Elevation	0.14	0.20	0.50	0.33	0.50	1	2
Distance to streams	0.14	0.20	0.50	0.33	0.50	0.20	1
Sum	2.4	5.43	10.83	11	15	20.5	22

Table 5. Physical parameters pairwise comparison matrix for scenario-2.

Parameter	Rainfalls	Elevation	Lithology	Land use	Type of soils	Distance to streams	Slope
Rainfalls	1	3	3	5	5	7	7
Elevation	0.33	1	2	3	3	5	7
Lithology	0.33	0.50	1	3	3	5	7
Land use	0.20	0.33	0.33	1	4	3	5
Type of soils	0.20	0.33	0.33	0.25	1	2	5
Distance to stream	0.14	0.20	0.20	0.33	0.50	1	3
Slope	0.14	0.14	0.14	0.20	0.20	0.33	1
Sum	2.35	5.51	7.01	12.78	16.70	23.30	35

Table 6. Physical parameter normalized matrix scenario-1.

Parameters	Slope	Rainfalls	Land use	Lithology	Type of soils	Elevation	Distance to streams	Sum	Mean
Slope	0.42	0.55	0.28	0.36	0.33	0.34	0.32	2.60	0.37
Rainfalls	0.14	0.18	0.46	0.18	0.20	0.25	0.23	1.64	0.23
Land use	0.14	0.04	0.09	0.27	0.13	0.10	0.09	0.86	0.12
Lithology	0.10	0.09	0.03	0.09	0.20	0.15	0.14	0.80	0.11
Type of soils	0.08	0.06	0.05	0.03	0.07	0.10	0.09	0.48	0.07
Elevation	0.06	0.04	0.05	0.03	0.03	0.05	0.09	0.35	0.05
Distance to streams	0.06	0.04	0.05	0.03	0.03	0.02	0.05	0.28	0.04
Sum	1.0	1.0	1.0	1.0	1.0	1.0	1.0	7.00	1.0

Table 7. Physical parameter normalized matrix scenario-2.

Parameter	Rainfalls	Elevation	Lithology	Land use	Type of soils	Distance to streams	Slope	Sum	Mean
Rainfalls	0.43	0.54	0.43	0.39	0.30	0.30	0.20	2.59	0.37
Elevation	0.14	0.18	0.29	0.24	0.18	0.21	0.20	1.44	0.21
Lithology	0.14	0.09	0.14	0.24	0.18	0.21	0.20	1.20	0.17
Land use	0.08	0.06	0.05	0.08	0.24	0.13	0.14	0.78	0.11
Type of soils	0.08	0.06	0.05	0.02	0.06	0.09	0.14	0.50	0.07
Distance to streams	0.06	0.04	0.03	0.03	0.03	0.04	0.08	0.31	0.04
Slope	0.06	0.03	0.02	0.02	0.01	0.01	0.03	0.18	0.03
Sum	1.0	1.0	1.0	1.0	1.0	1.0	1.0	7.00	1.0

The Pairwise Comparison Matrix and Weighted Parameters

Two sets of weighted parameters were used for the flooding vulnerability model in the Cilemer and Ciliman Watersheds. Visualizations of the models and their validation of the point flood history are shown in Figure 4a and 4b. The flood vulnerability models were calculated using Equation 3, and the vulnerability categories were represented by low, moderate, high, and very high vulnerabilities. These models were validated based on flooding history in the watershed. The results showed that there were 17 points from 31 points flooding occurrences in the high and very high vulnerability in scenario-1. Meanwhile, there were 19 points from 31 points flooding occurrences in the very high vulnerability in scenario-2. The two-point locations differ (purple squares), as shown in Figure 4a and 4b.

Within the weighted parameters in the two scenarios, the elevation and slope showed significant differences. The elevation weighted in scenario-1 is 0.05 and, 0.21 scenario-2. The slope weighted in scenario-1 is 0.37 and, 0.03 scenario-2. These differences influenced the validation of the point flood history. The two-point locations in scenario-2 are in the very high vulnerability area, while in scenario-1 both points are not in the area. Elevation and slope play an important role in governing the stability of a terrain. The slope affects the amount and direction of surface runoff at a site. Slope also has a dominant effect on the contribution of rainfall to streamflow, and it controls the duration of overland flow, infiltration, and subsurface flow [33,34].

Low-gradient slopes are more vulnerable to flooding than high-gradient slopes. Rain or excessive water from the river always accumulates in areas where the slope gradient is usually low. Areas with high slope gradients do not permit water accumulation, resulting in flooding. In this study, a slope map was prepared using a digital elevation model (DEM) and slope-generation tools using GIS software. The slope classes with lower

values were assigned a higher rank because of the almost flat terrain, whereas the class with the maximum value was categorized as a lower rank due to relatively high run-off (Table 2; Figure 3b). The very high vulnerability of the slope was mostly observed in the western area of the study. Flood occurrence points also existed in the western area of this study. However, a very vulnerable slope occurs in a very small area and does not cover flood points. Hence, the slope weighted in scenario-2 is rank last, and the elevation ranks second at the top. This condition causes the elevation to dominate the vulnerability calculation and influences the validation between the flood point history and flood vulnerability.

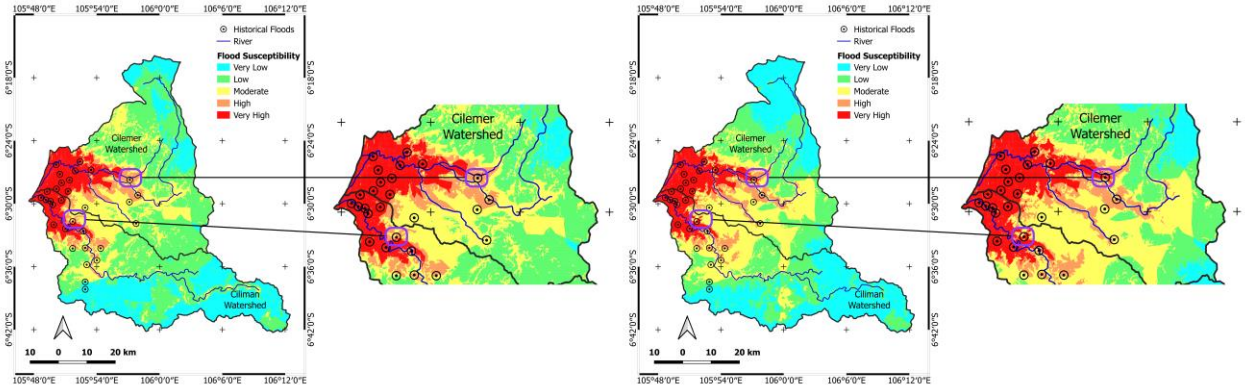

(a) (b)

Figure 4. Flood vulnerability models: (a) Scenario-1, and (b) Scenario-2.

Despite the systematic mapping and analysis of the parameters influencing flood areas, our study faced significant challenges owing to various limitations. Therefore, several aspects should be considered in future studies. The limitations are:

(i) The details of the DEMs data for river cells and their surrounding areas are limited. Hence, it is difficult to understand the situation of the river cells and the effectiveness of the distance to the river (streams) parameter in the potential flood maps.

(ii) To generate data driven by the pairwise comparison from historical flood occurrences in high and very high vulnerability areas, we can only estimate the value of data without further analysis of the influence of the potential flood parameters. This was demonstrated by our elevation parameters. Therefore, the pairwise in the second scenario needed to be combined with the expert judgment of each parameter influencing the potential flood.

(iii) Improving flood inventory data using satellite images of the location can be useful, as this method has not yet been used in our study.

Nonetheless, conducting a more comprehensive assessment of flood potentiality by utilizing higher-resolution data and advanced methods such as modern machine learning or statistical techniques may yield a more accurate flood map for the Cilemer and Ciliman Watersheds.

Conclusion

This study aims to assess two scenarios of potential flood vulnerability in the Ciliman and Cilemer Watersheds in the Pandeglang and Lebak Regencies of Banten Province, utilizing a spatial multi-criteria-integrated approach, specifically the Analytical Hierarchy Process (AHP). The two scenarios have different parameter priorities and their pairwise comparisons also differ. In scenario-1, parameter priority is based on expert judgment, while scenario-2 relies on the historical data of flooding occurrences in high and very high vulnerability areas. We found that the weighted parameters contributing to flood vulnerability in the two scenarios differed, leading to variations in the mapping of potential floods. In scenario-1, elevation and slope had the highest weights, whereas in scenario-2, rainfall and elevation were prioritized. Elevation and slope were consistently identified as crucial factors influencing the flood vulnerability in both scenarios. The validation of the two flood vulnerability mapping scenarios using historical flood data showed that scenario-2 exhibited closer agreement with the historical flood points during validation, particularly in areas with very high vulnerability. Our study suggests that more detailed data, particularly Digital Elevation Models (DEMs)

of river cells and surrounding areas, could improve the accuracy of flood vulnerability assessments, especially in areas prone to river overflow during heavy rainfall. Overall, further research and data refinement can enhance the precision of such assessments and contribute to effective flood management and mitigation strategies, specifically for the Ciliman and Cilemer Watersheds.

Author Contributions

DNH: Conceptualization, Methodology, Investigation, Writing - Review and Editing; **DP**: Data Processing.

Conflicts of interest

There are no conflicts to declare.

Acknowledgements

The authors gratefully acknowledged the publication funding by the Institute of Research and Community Service (LPPM), Institut Teknologi Nasional (Itenas)-Bandung, Indonesia.

References

1. Rogger, M.; Agnoletti, M.; Alaoui, A.; Bathurst, J.C.; Bodner, G.; Borga, M.; Chaplot, V.; Gallart, F.; Glatzel, G.; Hall, J.; et al. Land-use change impacts on floods at the catchment scale – challenges and opportunities for future research. *Water Resour. Res.* **2017**, *53*, 5209–5219.
2. Mengistu, T.D.; Chung, I.-M.; Kim, M.-G.; Chang, S.W.; Lee, J.E. Impacts and implications of land use land cover dynamics on groundwater recharge and surface runoff in East African watershed. *Water* **2022**, *14*, 1–18, doi:10.3390/w14132068
3. Gan B.R.; Liu X.N.; Yang X.G.; Wang X.K.; Zhoua J.W. The impact of human activities on the occurrence of mountain flood hazards: Lessons from the 17 August 2015 flash flood/debris flow event in Xuyong Country, South-Western China. *Geomat. Nat. Hazards Risk*. **2018**, *9*, 816–840.
4. Miardini, A.; Saragih, G.S. Penentuan Prioritas penanganan banjir genangan berdasarkan tingkat kerawanan menggunakan topographic wetness index: Studi kasus di DAS Solo. *Jurnal Ilmu Lingkungan* **2019**, *17*, 113–119, doi:10.14710/jil.17.1.x113-119.
5. Rimba, A.B.; Setiawati, M.D.; Sambah, A.B.; Miura, F. Physical flood vulnerability mapping applying geospatial techniques in Okazaki City, Aichi Prefecture, Japan. *Urb. Sci*. **2017**, *1*, 1–22, https://doi.org/10.3390/urbansci1010007.
6. BNPB (Badan Nasional Penanggulangan Bencana). Geoportal Data Bencana Indonesia. 2024. Available online: https://gis.bnpb.go.id (accessed on 26 August 2024).
7. Kristofery, L.; Murtilaksono, K.; Baskoro, D.P.T. Simulasi Perubahan penggunaan lahan terhadap karakteristik hidrologi Daerah Aliran Sungai Ciliman. *Jurnal Ilmu Tanah Dan Lingkungan* **2019**, *21*, 66–71.
8. Roy, D.C.; Blaschke, T. Spatial vulnerability assessment of floods in the coastal regions of Bangladesh. *Geomatics, Nat. Hazards Risk* **2015**, *6*, 21–44, doi:10.1080/19475705.2013.816785.
9. Mujib, M.; Apriyanto, B.; Kurnianto, F.; Ikhsan, F.; Nurdin, E.; Pangastuti, E.; Astutik, S. Assessment of flood hazard mapping based on Analytical Hierarchy Process (AHP) and GIS: Application in Kencong District, Jember Regency, Indonesia. *Geosfera Indonesia* **2021**, *6*, 353–376.
10. Saaty, T.L. *The Analytic Hierarchy Process: Planning, Priority Setting, Resource Allocation*; McGraw-Hill Book: New York, USA, 1980; pp. 287.
11. Xu, Z.; Liao, H. Intuitionistic fuzzy analytic hierarchy process. *IEEE Transactions on Fuzzy Systems* **2014**, *22*, 749–761.
12. BNPB (Badan Nasional Penanggulangan Bencana). Dokumen Kajian Risiko Bencana Kabupaten Pandeglang 2014-2018. 2014. Available online: https://inarisk.bnpb.go.id/pdf/BANTEN/Dokumen%20KRB%20PANDEGLANG_final%20draft.pdf (accessed on 13 March 2023).

13. Ramadhani, D.; Hariyanto, T.; Nurwatik. Penerapan metode analytical hierarchy process (AHP) dalam pemetaan potensi banjir berbasis Sistem Informasi Geografis (Studi kasus: Kota Malang, Jawa Timur). *Journal of Geodesy and Geomatics* **2021**, *17*, 72–80.
14. Wigati, R.; Arifin, F.S.; Lestari, M.D. Analisis banjir Sub DAS Cilemer HM 0+00 – HM 53+00. *Jurnal Ilmiah Rekayasa Sipil* **2020**, *17*, 134–143, doi:10.30630/jirs.12.2.388.
15. Dinas PUPR (Dinas Pekerjaan Umum dan Perumahan Rakyat) Banten. *Kajian Evaluasi Kinerja Penyelesaian Pengendalian Banjir DAS Cilemer*; Dinas PUPR Banten: Banten, ID, 2015;
16. Slamet, N.S.; Sarwono. Simulasi genangan banjir menggunakan data ASTER DEM pada aliran Sungai Cilemer. *J. Sumber Daya Air* **2016**, *12*, 61–67.
17. Cagla, M.K.; Leyla, D. Parameters and methods used in flood susceptibility mapping: A review. *Journal of Water and Climate Change* **2023**, *14*, 1935–1960, doi:10.2166/wcc.2023.035.
18. Handiani, D.N.; Heriati, A.; Gunawan, W.A. Comparison of coastal vulnerability assessment for Subang Regency in North Coast West Java-Indonesia. *Geomatics, Natural Hazards and Risk* **2022**, *13*, 1178–1206, doi:10.1080/19475705.2022.2066573.
19. Saaty, T.L.; Vargas, L.G. *Models, Methods, Concepts and Applications of the Analytic Hierarchy Process*; Kluwer Academic Publishers: Dordrecht, Netherlands, 2001; ISBN 978-1-4615-1665-1.
20. Dahri, N.; Habib, A. Monte Carlo simulation-aided analytical hierarchy process (AHP) for flood susceptibility mapping in Gabes Basin (Southeastern Tunisia). *Environ Earth Sci* **2017**, *76*, 1–14, doi:10.1007/s12665-017-6619-4.
21. Kazakis, N.; Kougias, I.; Patsialis, T. Assessment of flood hazard areas at a regional scale using an index-based approach and Analytical Hierarchy Process: Application in Rhodope–Evros region. *Greece. Sci. Total Environ*. **2015**, *538*, 555–563, doi:10.1016/j.scitotenv.2015.08.055.
22. Cabrera, J.S.; Lee, H.S. Flood-prone area assessment using GIS-based multi-criteria analysis: A case study in Davao Oriental, Philippines. *Water* **2019**, *11*, 1–23, doi:10.3390/w11112203.
23. Das, S.; Pardeshi, S.D.; Kulkarni, P.P.; Doke, A. Extraction of lineaments from different azimuth angles using geospatial techniques: A case study of Pravara basin, Maharashtra, India. *Arab J Geosci.* **2018**, *11*, 1–13, doi:10.1007/s12517-018-3522-6.
24. Das, S. Geospatial mapping of flood susceptibility and hydro-geomorphic response to the floods in Ulhas basin, India. *Remote Sensing Applications: Society and Environment* **2018**, *14*, 60–74, doi:10.1016/j.rsase. 2019.02.006.
25. Bui, D.T.; Pradhan, B.; Nampak, H.; Bui, Q.T.; Tran, Q.A.; Nguyen, Q.P. Hybrid artificial intelligence approach based on neural fuzzy inference model and metaheuristic optimization for flood susceptibility modeling in a high-frequency tropical cyclone area using GIS. *J Hydrol.* **2016**, *540*, 317–330, doi:10.1016/j.jhydrol.2016.06.027.
26. Rendana, M.; Idris, W.M.R.; Rahim, S.A.; Rahman Z.A; Lihan, T. Predicting soil erosion potential under CMIP6 climate change scenarios in the Chini Lake Basin, Malaysia. *Geosci. Lett*. **2023**, *10*, 1–16, doi:10.1186/s40562-022-00254-7.
27. Benito, G.; Ballesteros-Cánovas, J.A.; Díez-Herrero, A. Chapter 2 - Paleoflood hydrology: Reconstructing rare events and extreme flood discharges. In *Hydro-Meteorological Hazards, Risks, and Disasters*, 2nd ed.; Shroder, J.F., Paron, P., Di Baldassarre, G., Eds.; Elsevier: Amsterdam, Netherlands, 2023; Volume 5, pp. 33–83, ISBN: 978-0-12-819101-9.
28. Wilhelm, B.; Benjamin, A.; Juan, P.C.; William, R.; Charline, G.C.; Bruno, M.; Eivind, S. Reconstructing paleoflood occurrence and magnitude from lake sediments. *Quaternary* **2022**, *5*, 1–31, doi:10.3390/quat5010009.
29. Simamora, W.H. Anomali geomagnet, kaitannya dengan zone mineralisasi di daerah Malingping, Bayah, dan sekitarnya, Kabupaten Lebak, Provinsi Banten. *Jurnal Sumber Daya Geologi* **2006**, *16*, 285–301.
30. García-Ruiz, J.M.; López-Moreno, J.I.; Vicente-Serrano, S.M.; Lasanta–Martínez, T.; Beguería, S. Mediterranean water resources in a global change scenario. *Earth-Science Reviews* **2011**, *105*, 121–139, doi:10.1016/j.earscirev.2011.01.006.
31. Kourtis, I.M.; Tsihrintzis, V.A. Adaptation of urban drainage networks to climate change: A review. *Sci. Total Environ*. **2021**, *771*, 1–17, doi:10.1016/j.scitotenv.2021.145431.

32. Miranda, F.; Franco, A.B.; Rezende, O.; da Costa, B.B.F.; Najjar, M.; Haddad, A.N.; Miguez, M. A GIS-based index of physical susceptibility to flooding as a tool for flood risk management. *Land* **2023**, *12*, 1–22, doi:10.3390/land12071408.

33. Ouma, Y.O.; Tateishi, R. Urban flood vulnerability and risk mapping using integrated multi-parametric AHP and GIS: Methodological overview and case study assessment. *Water* **2014**, *6*, 1515–1545, doi:10.3390/ w6061515.

34. Wang, C.; Shang, S.; Jia, D.; Han, Y.; Sauvage, S.; Sánchez-Pérez, J.-M.; Kuramochi, K.; Hatano, R. Integrated effects of land use and topography on streamflow response to precipitation in an agriculture-forest dominated northern watershed. *Water* **2018**, *10*, 1–21, doi:10.3390/w10050633.